ROBUST DESIGN OF HIGH GAIN AMPLIFIERS USING DYNAMICAL SYSTEMS AND BIFURCATION THEORY

Chengming He, Le Jin, Degang Chen, Randall Geiger

Iowa State University, Ames, IA 50011 USA

ABSTRACT

An infinite DC gain CMOS positive feedback amplifier with 90° phase margin was designed and its nonlinear dynamics was studied using level 1 MOS models. Analytical derivations were utilized to investigate its equilibrium point, turning point, stability and branching properties. Analysis suggested this amplifier would show parameter-dependent supercritical pitchfork bifurcation. Bifurcation signals the instability of this amplifier when positive feedback factor is large. By decreasing the parameter until the bifurcation was eliminated, an amplifier with an infinite DC gain at operating-point was theoretically designed. Branching diagram was presented with numerical simulation. Gain nonlinearity was explained and methods to decrease this nonlinearity were proposed. Circuit simulations results verified our derivations.

1. INTRODUCTION

Amplifier design is as old as analog circuit design and MOS amplifier design may even be older than planar processes. Although MOS fabrication technologies have advanced as Moore's Law [1] predicted during the past four decades, analog circuit design did not evolve too much. Feature size shrinking [2] in advanced CMOS technology brought digital circuits great advantages, such as high integration, high speed, low power, and low cost. This progress helped to enhance some analog circuits' performances; nevertheless, it posed a great challenge to analog circuit design. Fast supply voltage drop and slow threshold voltage drop greatly limited traditional high gain amplifier structures to achieve large output swings. A positive feedback amplifier has the potential to provide low-voltage compatibility, large output swings and good frequency response [3]. However, it behaves much more like a nonlinear circuit though it is supposed to be a 'linear' device. A few works tried to limit its gain-nonlinearity but few achieved good results [3, 4, 5].

Traditional circuit designers typically used small signal equivalent linear models [6, 7] to study analog circuits or even call those circuits 'linear circuits'. However, nonlinearity in circuits becomes more apparent with feature size shrinking [7]. Linear models are still valid in certain applications. However, these models cannot explain gain nonlinearity and some special dynamics (e.g., hysteresis) shown in some 'not-well-designed' positive feedback amplifiers. Thus, it is important to use nonlinear system dynamics to study the positive feedback amplifier. Nonlinearity may either benefit or hurt a circuit's performance. After we understand the nonlinearity in analog circuits, we can choose to utilize the advantages while avoiding the disadvantages.

In this paper, a positive feedback amplifier's system dynamics were studied. Section 2 introduces bifurcation phenomenon in nonlinear dynamical systems [8]. Section 3 provides analytical derivations of dynamical behavior in a traditional differential amplifier and in a positive feedback amplifier [5]. Parameter dependency of bifurcation [8] is used to study the positive feedback amplifier. Some interesting properties were discovered and used to maintain a high DC gain. Gain nonlinearity was explained in our derivations. Branching diagram was obtained by numerical simulations. Section 4 presented transistor-level circuit simulations results, which verified the analytical derivations. Conclusions were given in section 5.

2. BIFURCATION IN DYNAMICAL SYSTEMS

Bifurcation [8] is one commonly encountered nonlinear phenomenon in dynamical systems. It is characterized by bifurcation points and branches, as shown in Fig. 1. A bifurcation point is easy to characterize geometrically: at a bifurcation point, two branches with distinct tangents intersect. Fig. 1 shows a branching diagram of pitchfork bifurcation. Pitchfork includes supercritical pitchfork and subcritical pitchfork but we will only focus on supercritical pitchfork in this paper.

We will explain supercritical pitchfork concisely and define some terms that used in the paper. First, let us go through a differential equation (1)

$$\dot{y} = (\mu - \mu_0)y - y^3 \qquad (1)$$
$$\mu_0 = Cons\tan t; \mu_0, \mu, y \in R$$

Equation (1) is a model of supercritical pitchfork.

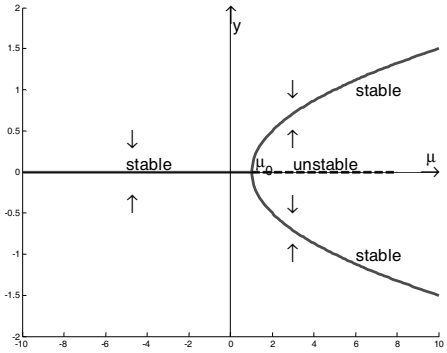

Fig. 1 pitchfork bifurcation

For $\mu > \mu_0$, there are two stable equilibria, $y = \pm\sqrt{\mu - \mu_0}$ and an unstable equilibrium $y_0 = 0$. For $\mu \le \mu_0$, there is only one stable equilibrium at $y_0 = 0$. We call point (y_0, μ_0) a bifurcation point and μ branching parameter. Fig. 1 shows the branch diagram of this supercritical pitchfork bifurcation.

3. SYSTEM DYNAMICS IN TWO AMPLFIERS

3.1. A Fully Differential Amplifier

The circuit shown in Fig. 2a is used as a fully differential amplifier in analog VLSI [6]. Assume it has perfect symmetry, we can use the equivalent linear model depicted in Fig. 3b to analyze frequency response. The model is obtained by locally linearizing the circuit at its operating point, i.e., $V_{i1} = V_{i2} = V_{ICM}$ and $V_{o1} = V_{o2} = V_{oCM}$.

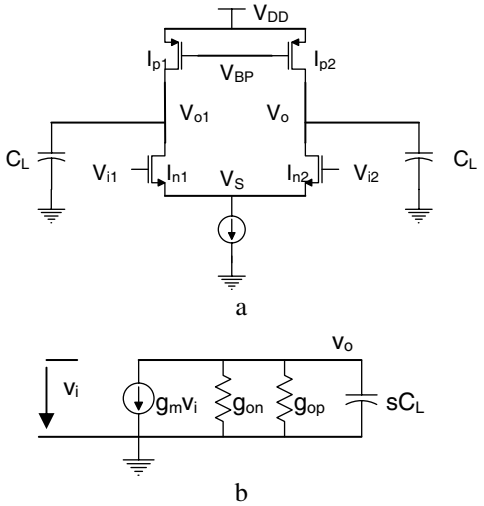

Fig. 2 A fully differential amplifier and its equivalent linear model

Analog circuit designers are more interested in the situation when all transistors are in saturation region. We will focus on this situation. Instead of using locally linearized model to analyze this circuit, however, we will use differential equations to study the dynamic of this circuit, which includes stability of operation point (an equilibrium point).

Without loss of validity, MOS level 1 I_{DS} Schichman-Hodges model [9] is used to derive the system dynamics. In this model $I = \beta V_{EB}^2 (1 + \lambda |V_{DS}|)$.

After careful derivations, we found differential equation (2) denoting this amplifier's system dynamics.

$$\frac{dv_o}{dt} = -\frac{(\beta_p V_{EBP}^2 \lambda_p + \beta_n V_{EBN}^2 \lambda_n)}{C_L} v_o - \frac{\beta_n \lambda_n [1 + \lambda_n (V_{OCM} - V_S)] v_i^2}{4 C_L} v_o - \frac{2\beta_n V_{EBN} [1 + \lambda_n (V_{OCM} - V_S)]}{C_L} v_i \quad (2)$$

Denote $y = v_o$, $x = v_i$, $g_{op} = \lambda_p \beta_p V_{EBP}^2$, $g_{on} = \lambda_n \beta_n V_{EBN}^2$, $g_{mn} = 2\beta_n V_{EBN} [1 + \lambda_n (V_{OCM} - V_S)]$

Rewrite the differential equation (2) as equation (3).

$$\dot{y} = -\frac{g_{op} + g_{on}}{C_L} y - \frac{\beta_n \lambda_n [1 + \lambda_n (V_{OCM} - V_S)] x^2}{4 C_L} y - \frac{g_{mn}}{C_L} x = a(x) y - bx = f(x, y) \quad (3)$$

Under normal operating range, $a(x) < 0$. This suggests this system is always stable and $y = 0$ is the sole stable equilibrium point when there is no excitation.

In circuit design field, DC gain (including magnitude and phase) at operating point is defined as the slope of $f(x, y)$ at the equilibrium point (0,0), which is

$$A\big|_{(0,0)} = \frac{f_x(0,0)}{f_y(0,0)} = -\frac{g_{mn}}{g_{op} + g_{on}} \quad (4)$$

3.2 System dynamics of a Positive feedback amplifier

Fig. 3 depicts a positive feedback amplifier [5]. Unlike traditional positive feedback amplifiers, its system dynamics is controlled by feedback factor.

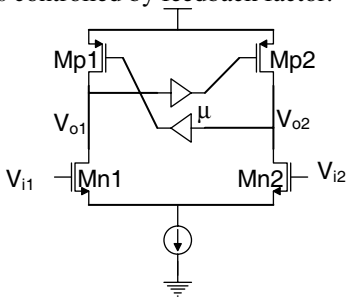

Fig. 3 A positive feedback amplifier

Unlike the circuit in Fig. 2, the gates of PMOS transistors are connected to output through a feedback buffer with attenuation of μ. This circuit has the same operating point as the circuit shown in Fig. 2a.

Using the same denotation, we get differential equation (5) representing the dynamics of this new circuit.

$$\begin{aligned} C_L \frac{dv_{o1}}{dt} &= \beta_p (V_{EBP} - \mu v_{o2})^2 [1 + \lambda_p (V_{DD} - V_{OCM} - v_{o1})] \\ &\quad - \beta_n (V_{EBN} + v_{i1})^2 [1 + \lambda_n (V_{OCM} + v_{o1} - V_S)] \\ C_L \frac{dv_{o2}}{dt} &= \beta_p (V_{EBP} - \mu v_{o1})^2 [1 + \lambda_p (V_{DD} - V_{OCM} - v_{o2})] \\ &\quad - \beta_n (V_{EBN} + v_{i1})^2 [1 + \lambda_n (V_{OCM} + v_{o2} - V_S)] \end{aligned} \quad (5)$$

Let $v_{i1} = -v_{i2} = \frac{v_i}{2}$, under the assumption of perfect symmetry, we can get $v_{o1} = -v_{o2} = \frac{v_o}{2}$.

Let $x = v_i, y = v_o$, the partial differential equations (5) can be rewritten as (6).

$$\dot{y} = -\frac{g_{op} + g_{on} - \mu g_{mp}}{C_L} y - \frac{\mu^2 \beta_p \lambda_p}{4C_L} y^3 - \frac{\beta_n \lambda_n [1 + \lambda_n (V_{OCM} - V_S)] x^2}{4C_L} y - \frac{g_{mn}}{C_L} x \quad (6)$$

We first investigate the stability of deflection when x=0, as depicted in equation (12)

$$\dot{y} = -\frac{g_{op} + g_{on} - \mu g_{mp}}{C_L} y - \frac{\mu^2 \beta_p \lambda_p}{4C_L} y^3 = f(y, \mu) \quad (7)$$

Let $f(y, \mu) = 0$, it turns out that for $\mu > \frac{g_{op} + g_{on}}{g_{mp}}$ three are two stable equilibria with $y = \pm \sqrt{\frac{4(\mu g_{mp} - g_{op} + g_{on})}{\mu^2 \beta_p \lambda_p}}$ and one unstable equilibrium $y = 0$, whereas for $\mu \le \frac{g_{op} + g_{on}}{g_{mp}}$ there is solely one stable equilibrium $y = 0$.

Fig. 4 shows this branching diagram assuming the branching parameter have sufficient large variability. Fig. 4 depicts two possible branching diagrams, (a) without any constrains at output and (b) with saturation at outputs. The symmetry of the branching diagrams with respect to the μ-axis reflects the basic assumption of perfect symmetry.

This branching diagram has a branching point $(y_0, \mu_0) = (0, \frac{g_{op} + g_{on}}{g_{mp}})$. We can show the branching point $(0, \frac{g_{op} + g_{on}}{g_{mp}})$ is a bifurcation point.

Let's rewrite the differential equation (6) as

$$\dot{y} = -\frac{g_{op} + g_{on} - \mu g_{mp}}{C_L} y - \frac{\mu^2 \beta_p \lambda_p}{4C_L} y^3 - \frac{\beta_n \lambda_n [1 + \lambda_n (V_{OCM} - V_S)] x^2}{4C_L} y - \frac{g_{mn}}{C_L} x = f(y, x, \mu) \quad (8)$$

Given μ known, equation $f(y, x, \mu) = 0$ tells the relationship between input x and output y, which is called a DC transfer characteristic in circuit design.

Based on the definition used in circuit design area, gain function (shown in equation 9) is the tangent of $f(y, x, \mu)$ in (y, x) plane.

$$\frac{f_x'}{f_y'} = -\frac{g_{mn} + co1 * xy}{g_{op} + g_{on} - \mu g_{mp} + \frac{3}{4}\mu^2 co2 * y^2 + \frac{co1}{2} x^2} \quad (9)$$

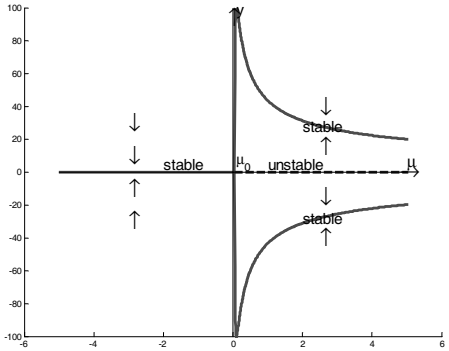

a

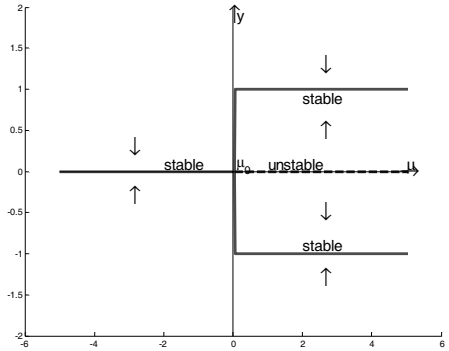

b

Fig. 4 Branching diagrams of PFA: (a) no constrain (b) saturation at output

For a high gain positive feedback amplifier, feedback factor μ is ideally set to be $\mu_0 = \frac{g_{op} + g_{on}}{g_{mp}}$. This amplifier achieves an infinite DC gain at bifurcation point $(0,0, \frac{g_{op} + g_{on}}{g_{mp}})$ but gain drops in a speed proportional to y^{-2}. This explains high gain nonlinearity in most positive feedback amplifiers. In order to limit this non-linearity, small λ is preferred which suggests wide length transistors.

When $\mu < \frac{g_{op} + g_{on}}{g_{mp}}$ there exists a one-one mapping between y and x solving the equation $f(y, x, \mu) = 0$. The solution for $f(y, x, \mu) = 0$ becomes complex when $\mu \ge \frac{g_{op} + g_{on}}{g_{mp}}$. One-One mapping from x to y turns to be invalid. Given μ fixed, there exists a boundary $x_0 > 0$ for bifurcation. When $|x| < x_0$, we can find two stable equilibria and an unstable equilibrium. When $|x| > x_0$, there will be only one stable equilibrium point. x_0 is given by a solution of equation (8) and (10)

$$\frac{\partial f(y,x,\mu)}{\partial y} = -\frac{g_{op} + g_{on} - \mu g_{mp}}{C_L} - \frac{3\mu^2\beta_p\lambda_p}{4C_L} y^2 - \frac{\beta_n\lambda_n[1+\lambda_n(V_{OCM} - V_S)]x^2}{4C_L} = 0 \quad (10)$$

One will get equation (11) combining equation (8) and (10).

$$(g_{op} + g_{on} - \mu g_{mp}) + \frac{3\mu^2\beta_p\lambda_p}{4}\left(\frac{2x}{\mu^2\beta_p\lambda_p}\right)^{2/3} + \frac{\beta_n\lambda_n[1+\lambda_n(V_{OCM} - V_S)]x^2}{4} = 0 \quad (11)$$

One can get an analytical expression for x_0 with the knowledge of general method to cubic equations. Equation 12 gives an estimation on the upper bound of x_0.

$$x_0 \le \frac{2(\mu g_{mp} - g_{op} - g_{on})^{3/2}}{3\sqrt{3\mu^2\beta_p\lambda_p}}$$

$$x_0 \le \sqrt{\frac{4(\mu g_{mp} - g_{op} - g_{on})}{\beta_n\lambda_n[1+\lambda_n(V_{OCM} - V_S)]}} \quad (12)$$

In order to observe bifurcation, one has to limit excitation to be a small value especially when μ is close μ_0. Fig. 5 shows the branching diagram respect to excitation x for different branching parameters. Depending on μ, DC transfer characteristics may display hysteresis or not. An infinite DC gain exists at the bifurcation point.

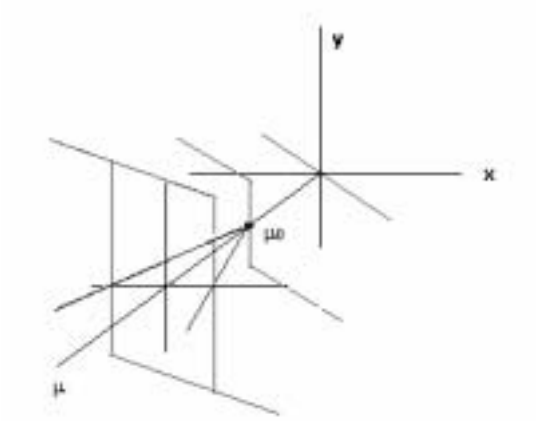

Fig. 5 DC transfer characteristics of different control factors

4. CIRCUIT SIMULATION RESULTS

Digital CMOS transistors were used to realize both amplifiers. Gain nonlinearity and bifurcation was observed in the positive feedback amplifier. After canceling bifurcation by adjusting the control factor, the amplifier achieved an infinite DC gain at operating point. Table 1 summarized performances of these two amplifiers shown in Fig. 2 and 3. Without scarifying power, positive feedback amplifier achieves much higher gain. Simulations covering full corners over a wide temperature range were conducted and nearly all achieved above 80dB gain, which validated our derivations. This suggests this amplifier has the potential to achieve high yield.

Table 1 Performance of circuits in Fig. 2 and Fig. 3

	Fig. 2	Fig. 3
Tail current	I	I
DC Gain	$\frac{g_m}{g_{on} + g_{op}}$	∞
GBW(C_L)	$\frac{g_m}{C_L}$	$\frac{g_m}{C_L}$
Phase Margin	90°	90°

5. CONCLUSIONS

Dynamical systems and bifurcation theory are introduced to explain nonlinearity in analog circuits and a new design method was used in addition to classical analog circuit design, which enhances analog performance dramatically. We have successfully achieved an infinite DC gain amplifier using bifurcation theory, which is impossible to obtain using traditional circuit design knowledge. Beginning with traditional circuit design techniques, utilizing dynamical systems and bifurcation theory, we developed a robust design method for high gain low-voltage compatible amplifiers with expected high yield in digital CMOS.

6. REFERENCES

[1] G. E. Moore, "Cramming more Components onto Integrated Circuits," *Electronics*, vol. 38, no. 8, April 19, 1965.

[2] X. Huang, et al. "Sub 50-nm FinFET: PMOS," *Technical Digest of International Electron Devices Meeting*, pp. 67-70, Dec. 1999.

[3] J. Yan and R. L. Geiger, "A high gain CMOS operational amplifier with negative conductance gain enhancement", *IEEE Proc. of Custom Integrated Circuits Conf.*, Orlando, FL, USA 2002, pp. 337-340.

[4] M. Schlarmann, S. Q. Malik and R. L. Geiger, "Positive Feedback Gain Enhancement Techniques for Amplifier Design," *Proc. of 2002 ISCAS*, vol. 2 Phoenix, May 2002, pp. 37-40.

[5] Chengming He, D. Chen and R. L. Geiger, "A Low-Voltage Compatible Two-Stage Amplifier with ≥120dB Gain in Standard Digital CMOS," *Proceedings of 2003 ISCAS*, Vol. 1 , Bangkok, Thailand, May 2003, pp. 353-356.

[6] D. Johns and K. Martin, *Analog Integrated Circuit Designs*. New York: Wiley, 1997.

[7] Behzad Razavi, *Design of Analog CMOS Integrated Circuits*. McGraw-Hill, 2001.

[8] R. Seydel, *From Equilibrium to Chaos: Practical bifurcation and stability analysis*. New York: Elsevier Science Publishing co., Inc, 1988, CH. 2.

[9] Met-Software Inc., "HSPICE User's Manual," Meta-Software, Inc., HSPICE version H92, 1992.